Journal of Cellular Biochemistry 99:178–186 (2006)

In Vitro Toxicology Evaluation of Pharmaceuticals Using Raman Micro-Spectroscopy

Chris A. Owen, Jamuna Selvakumaran, Ioan Notingher, Gavin Jell, Larry L. Hench, and Molly M. Stevens*

Department of Materials, Imperial College London, South Kensington Campus, Exhibition Road, London SW7 2AZ, United Kingdom

Abstract Raman micro-spectroscopy combined with multivariate analysis was employed to monitor real-time biochemical changes induced in living cells in vitro following exposure to a pharmaceutical. The cancer drug etoposide (topoisomerase II inhibitor) was used to induce double-strand DNA breaks in human type II pneumocyte-like cells (A549 cell-line). Raman spectra of A549 cells exposed to 100 μM etoposide were collected and classical least squares (CLS) analysis used to determine the relative concentrations of the main cellular components. It was found that the concentrations of DNA and RNA significantly ($P < 0.05$) decreased, whilst the concentration of lipids significantly ($P < 0.05$) increased with increasing etoposide exposure time as compared to control untreated A549 cells. The concentration of DNA decreased by 27.5 and 87.0% after 24 and 48 h exposure to etoposide respectively. Principal components analysis (PCA) successfully discriminated between treated and untreated cells, with the main variance between treatment groups attributed to changes in DNA and lipid. DNA fragmentation was confirmed by Western blot analysis of apoptosis regulator protein p53 and cell metabolic activity determined by MTT assay. The over-expression of p53 protein in the etoposide treated cells indicated a significant level of DNA fragmentation and apoptosis. MTT tests confirmed that cellular metabolic activity decreased following exposure to etoposide by 29.4 and 61.2% after 24 and 48 h, respectively. Raman micro-spectroscopy may find applications in the toxicology screening of other drugs, chemicals and new biomaterials, with a range of cell types. J. Cell. Biochem. 99: 178–186, 2006.

Key words: Raman spectroscopy; pharmaceuticals; drug testing; etoposide; VP-16; apoptosis; toxicology

Adverse drug responses are associated with a large financial cost and account for 6.5% of hospital admissions and 0.15% fatalities making them between the 4th and 6th highest causes of death in the developed world (after heart disease, cancer and stroke) [Lazarou et al., 1998]. Furthermore, 51% of drugs that do not induce side effects in an animal model may result in serious side effects in humans [Moore et al., 1998]. There is thus a strong drive to develop in vitro technologies for more efficacious and economical pharmaceutical testing.

Raman spectroscopy is routinely used for the characterisation of different active groups, polymorphs and isomers within pharmaceuticals. We utilise it here for the in vitro toxicological evaluation of pharmaceuticals on live human cells, an application that has not yet received widespread attention. In vitro based toxicological testing systems based on drug interactions with human cells may ultimately provide valuable additional (and in some cases more predictive) drug safety data to testing in animals. The advantages of using Raman spectroscopy for the analysis of human cell: Drug interactions over using animal models are that it is very fast, has low operating costs and the results relate to human cells. This is a rapidly emerging application of Raman spectroscopy that is likely to yield additional predictive

Grant sponsor: Medical Research Council; Grant number: G010030; Grant sponsor: The US Defence Advanced Research Projects Agency (DARPA); Grant number: N66001-C-8041.

This article contains supplementary material, which may be viewed at the Journal of Cellular Biochemistry website at http://www.interscience.wiley.com/jpages/0730-2312/suppmat/index.html.

*Correspondence to: Molly M. Stevens, Department of Materials, Imperial College London, South Kensington Campus, Exhibition Road, London SW7 2AZ, UK.
E-mail: m.stevens@imperial.ac.uk

Received 31 January 2006; Accepted 13 February 2006

DOI 10.1002/jcb.20884

information to that generated by current animal methods. Conventional in vitro assays such as LDH (lactate dehydrogenase), MTT (3-(4,5-Dimethyl-2-thiazolyl)-2,5-diphenyl-2H-tetrazolium bromide), neutral red and live/dead are all destructive techniques. Raman microspectroscopy has a key advantage for studying living cells in vitro, namely that no labels or fixation are required. Furthermore, it is a non-destructive technique, enabling the same cell to be monitored in real-time over a series of different time points (e.g., analysing the action of a drug every 6 h for a week on the same cells). Furthermore, Raman measurements on cells can be performed in physiological-like conditions due to the low Raman signal of aqueous solutions (culture medium or buffer solutions). It is not only toxicology where Raman spectroscopy has benefits; evaluating the status of cells on novel substrates used in tissue-engineering over a period of time without destruction of the cells is also enabled by this technique.

Raman spectroscopy is based on the inelastic interaction between monochromatic electromagnetic radiation and the test sample [Raman and Krishnan, 1928]. The result is a spectrum that represents a chemical fingerprint of the sample. High resolution Raman spectroscopy studies have been conducted on chromosomes [Puppels et al., 1990], cytotoxic vesicles in killer T lymphocytes [Takai et al., 1997] and cholesterol crystals in endothelial cells [Hawi et al., 1997]. Cellular component distribution within living and fixed cells has been imaged using confocal Raman imaging [Uzunbajakava et al., 2003a,b; Krafft, 2004]. We have recently shown that biochemical changes related to cell death and stem cell differentiation can be monitored in real-time with this technique [Notingher et al., 2003; Verrier et al., 2004; Notingher et al., 2004a,b; Jell et al., 2006].

In order to investigate the use of Raman spectroscopy in toxicological testing using human cells, it must first be demonstrated that the technique can accurately monitor biochemical alterations in the cells when a chemical with a known effect is added. In this study, the cancer drug etoposide (topoisomerase II inhibitor) was used to induce double-strand DNA breaks in human type II pneumocyte-like cells (A549 cell-line). Etoposide is used to treat cancer of the windpipe (bronchus), lymphomas and testicular cancer, among others [RPSGB, 2002]. It induces double-stranded breaks in DNA by inhibiting topoisomerase II activity during DNA replication and thus targets cells that are dividing.

In this study, a classical least squares (CLS) model has been developed to interpret changes in the Raman spectral signatures of the A549 cells upon exposure to etoposide. In this model, the Raman spectrum of a sample is considered to be a linear combination of Raman spectra obtained from the pure chemical constituents of the sample. The developed CLS model uses commercially available biopolymers to model the key cellular components and allow determination of each chemical constituent using a least square fitting routine. The method is similar in principle to other CLS models that have been successfully applied to Raman spectra to determine the biochemical composition of breast tissue [Shafer-Peltier et al., 2002], skin [Caspers et al., 2001], arteries [Salenius et al., 1998] and fixed (dead) single cells [Krafft et al., 2005]. CLS analysis of Raman data collected from living single cells has yet to be described. Principal components analysis (PCA) is also applied to the data.

Biochemical changes detected by Raman spectroscopy are compared with results from MTT assay for cellular respiratory activity and the expression of p53, a protein that is up-regulated in response to DNA damage.

EXPERIMENTAL METHODS

Cellular Techniques

Human epithelial-like lung carcinoma cell line (A549) cells (ATCC) were cultured until 70% confluent in a 75 cm^2 flask in medium consisting of F12k medium with 10% foetal calf serum and 1% antibiotic-antimycotic (all from Invitrogen, UK) at 37°C and 5% CO_2. The cells were then trypsinised and diluted in medium to 10,000 cells/ml. Eighteen sterilised MgF_2 (magnesium fluoride) substrates were placed in individual wells in a 48 well plate and covered with 1 ml of the cell suspension. (MgF_2 substrates have previously been shown to have low ion solubility, a low Raman signal in the biological area of interest and allow good cell attachment [Notingher et al., 2004c]). The medium was aspirated after 8 h, the substrates washed with phosphate buffered saline (PBS) and fresh medium added. After 24 h, 6 cell-coated MgF_2 substrates were used for Raman spectroscopy analysis. The medium from the other 12 wells was aspirated and fresh medium

containing 100 μM etoposide (Sigma Aldrich, Dorset, UK) added. After 24 and 48 h etoposide exposure, 6 cell-coated MgF_2 substrates were removed for Raman spectroscopy analysis.

Raman Spectroscopy

The Raman system used consisted of a Renishaw RM 2000 spectrometer (Renishaw PLC, UK) connected to a Leica microscope with an immersion objective (63×). A 785 nm 300 mW line focus laser with 100 mW power at the sample was used. This wavelength and power is sufficient to produce a high signal to noise ratio Raman spectrum from a living cell without damaging the cell [Notingher et al., 2003]. The laser spot size was calculated to be 10 μm wide by 20 μm high and 40 μm deep. The spectrometer was set up with a spectrometer slit of 50 μm and 8 CCD (charge-coupled device) pixels.

The cell-coated MgF_2 substrates were covered in PBS and placed into custom designed chambers attached to the spectrometer that were maintained at 37°C throughout the experiments with a heated stage. Four 30 seconds spectra were taken per cell to cover the whole cell between Raman wave number shifts of 600 and 1,800/cm. Raman spectral analysis is capable of supplying more detailed information about the entire biochemical composition of a cell than traditional assays (such as MTT or LDH) in a shorter period of time. A minimum of 40 cells were analysed by Raman spectroscopy for each experimental condition and time point. The background spectrum of PBS was also taken for subtraction during spectral pre-processing.

Statistical Analysis

All statistical analyses on cells and cellular components were performed in Matlab® using functions developed by NovaThera® Ltd (London). The x-axis was standardised using a linear interpolation algorithm. The y-axis was calibrated using a glass reference spectrum taken on each experimental day. The PBS spectrum was subtracted using a subtraction algorithm previously described [Maquelin et al., 2002]. A Savitsky-Golay smoothing filter was applied to the spectra (21 points, 2nd order polynomial) and the second derivative was taken in order to remove the fluorescence background from the Raman spectra. The spectra were then scaled (normalisation) using the standard normal variate (SNV) transformation method where the average of the spectral intensities is set at 0 and the standard deviation is set to 1, as previously described [Barnes et al., 1989; Luypaert et al., 2004].

The primary cellular components used for CLS analysis were: Calf thymus DNA; bakers yeast RNA; phosphatidyl choline and cholesterol (lipids found in cell membranes); human serum albumin (high α-helix content protein); chymotrypsin (high β-pleated sheet content protein); actin; collagen and glycogen (all from Sigma Ltd, UK). In order to obtain an accurate CLS model, representatives of all major cellular biopolymers needed to be included. The nine components here represent nucleic acids, proteins, lipids and carbohydrates. For spectroscopic measurements, the chemicals were dissolved in PBS, except the lipids that were immersed in PBS. These cell components were pre-processed in the same way as the cells and then fitted using the CLS algorithm.

The overall accuracy of the CLS model was determined by dividing the difference between the CLS and actual peak intensities by 2 (±1 standard deviation) and multiplying by 100 (for each group). The accuracy of the CLS prediction of DNA was determined in the same way with the exception that we used the intensities of the actual and CLS-modelled peaks that are found in the DNA spectrum (based on the 22 most prominent peaks and troughs of the DNA spectrum as seen in Figure 2).

PCA was also performed on the smoothed cell spectra to calculate the variance between cell spectra in the form of principal components.

MTT Assay and Western Blot Analysis

The respiratory activities of the cells were assessed at the experimental time points using an MTT assay. Western blots were performed for the same time points using a modified version of the Laemmli protocol [Laemmli, 1970]. Briefly, cells were removed from the MgF_2 substrate by trypsinisation, diluted to equivalent cell densities after performing a cell count using a trypan blue assay and then centrifuged at 200 rpm for 8 min. The resulting pellet was lysed and a protein extraction kit (Novagen, UK) used to extract the cytoplasmic and nuclear proteins separately. The nuclear extracts were diluted with an equal volume of sample buffer and 5 μl loaded onto a 10% polyacrylamide gel along with an untreated cell

nuclear extract control and molecular weight marker. A constant voltage of 200 V for 40 min was applied before transferring to a polyvinylidene fluoride membrane overnight at 30 V constant voltage. The membrane was blocked by 2% w/v bovine serum albumin and p53 immunochemically detected with primary rat anti-human p53 antibody and secondary goat anti-rat IgG (both from Dako, Denmark), prior to detection with enhanced chemiluminescence.

RESULTS

Following 48 h exposure to etoposide, features symptomatic of cell death were observed. Namely, a number of cells became non-adherent and others were observed with modified morphology such as retracted membranes, fewer filopodia and a more rounded appearance. Some of the cells appeared large and flattened with visible nuclear fragmentation, characteristic of an apoptotic response to etoposide exposure in this cell type [Huang et al., 1997].

The Raman spectra of cells exposed to etoposide retained the peaks observed in untreated cells over the course of the study (Fig. 1A (spectra a, b and c)). The difference between the spectra of treated and untreated cells shows increasing differences upon increased exposure to etoposide indicating biochemical changes in the cells in response to the drug (Fig. 1A (spectra d, e and f)). From inspection of the differences spectra, the most noticeable peak changes were the increase of the 1,158 and 720/cm peaks that relate to CC stretching in lipids and the symmetric stretching of the choline group $CN^{+}(CH_3)_3$ in phosphatidyl choline, and the decrease in the 788/cm peak that relates to DNA. The differences in the 788/cm peak are shown in more detail in Figure 1B (spectra a, b and c). Raman spectral peaks and assignments relevant to cell spectral signatures can be found in the literature [Notingher et al., 2004a]. The differences observed in these spectra appear to be small and in order to make sense of such complex changes in the spectra, multivariate analysis methods were employed to extract information specific to the cellular biopolymers chosen for modelling.

The 2nd derivative Raman spectra of the cell components used to build the CLS model and a typical spectrum of an A549 cell are shown in Figure 2. The biopolymer cell component spectra showed a high degree of orthogonality

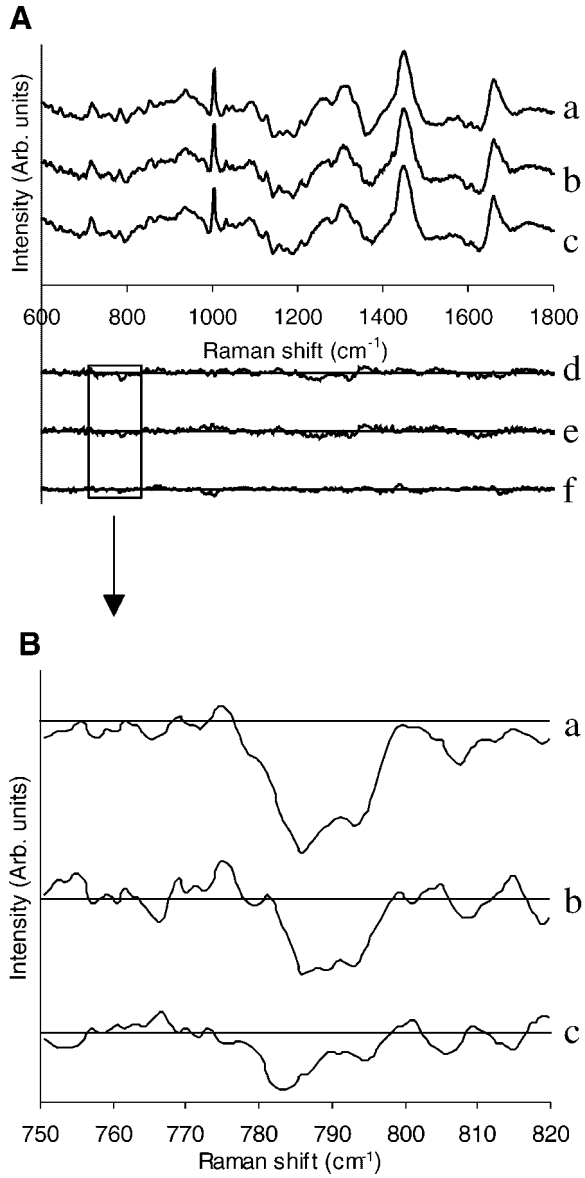

Fig. 1. **A**: Raman spectra of A549 cells. The top 3 are normalised spectra with PBS and fluorescence subtracted. The bottom 3 spectra show the spectral differences between the treated and untreated cells. The spectra have been shifted vertically for clarity: (a) Untreated cells; (b) 24 h after etoposide treatment; (c) 48 h after etoposide treatment; (d) Difference spectrum of 48 h treated—untreated cells; (e) Difference spectrum of 24 h treated—untreated cells; (f) Difference spectrum of 48 h treated—24 h treated cells. **B**: Detail around 788/cm peak for the difference spectra in (A). (a) Difference spectrum of 48 h treated—untreated cells; (b) Difference spectrum of 24 h treated—untreated cells; (c) Difference spectrum of 48 h treated—24 h treated cells.

(judged to be the case when the scalar product |k| is less than 0.1), with the exception of similarities between the α protein (HSA) and β protein (chymotrypsin) models and the other

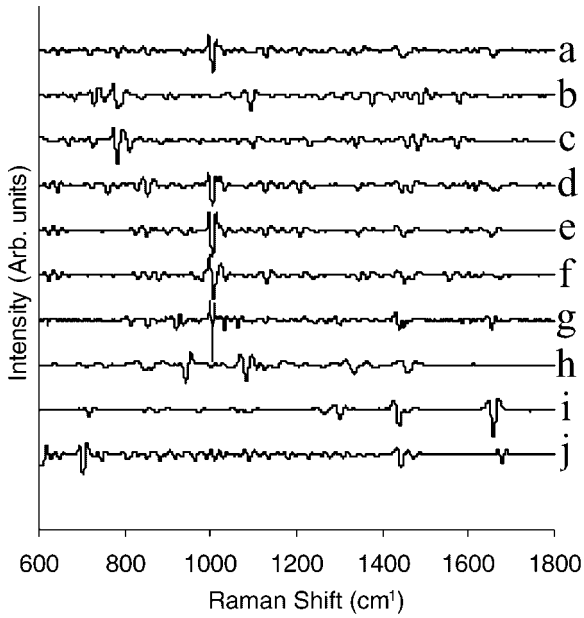

Fig. 2. Second derivative average Raman spectra of the A549 cells and the classical least squares (CLS) model components: (a) A549 cell spectra; (b) DNA; (c) RNA; (d) actin; (e) human serum albumin; (f) chymotrypsin; (g) collagen; (h) glycogen; (i) phosphatidyl choline; (j) cholesterol.

proteins actin and collagen and a lower level of similarity between DNA and RNA (Table I). The fitting of similar components (i.e., HSA and chymotrypsin) is likely to be less accurate and "total" protein levels are thus presented in this study. The total protein (mean of the four spectra used) spectrum is orthogonal to other components enabling a reliable estimation.

A good fit is observed between the developed CLS model spectrum and the average measured 2nd derivative spectrum of A549 cells (Fig. 3). Raman spectra of cells exposed to 100 μM etoposide reveal significant ($P < 0.05$) decreases in DNA concentration of 27.5 and 87.0% after 24 and 48 h respectively as calculated with the CLS model (Fig. 4). Significant ($P < 0.05$) decreases in RNA levels are also observed after 24 h. The overall level of protein in the cells did not vary significantly over a period of 48 h following exposure to etoposide. The concentration of phospholipids (modelled by phosphatidyl choline, a major component of cell membranes) increased significantly after 48 h exposure to etoposide.

The average inaccuracy of individual CLS-modelled peaks found in DNA was found to be 8.8, 11.7 and 12.3% for the untreated, 24 and 48 h groups. However, there was very little bias towards over or underestimating DNA levels as a whole. When the sign of the difference of each peak was taken into account, the average percentage inaccuracy becomes just 1.4, 0.4 and 4.3% for the 3 groups. In the same manner, the average inaccuracy of each individual Raman shift wave number was found to be 12.6, 16.3 and 13.4% for the 3 groups. There are some differences between the actual cell spectra and the CLS model, in particular at 720 and 1,440/cm, which are peaks that relate to lipids. This may suggest that the fit for lipids may not be as good as other components. However, for many other peaks relating to lipids an accurate fit is provided, such as the 1,301/cm (CH_2 twist), 877/cm (CCN^+ symmetric stretch) and 1,065/cm (CC stretch).

PCA was used to show a clear distinction between treated and untreated groups, as the scores for PC2 were higher for untreated

TABLE I. Orthogonality Degree |k| Between the 2nd Derivative Raman Spectra of the Pure Compounds Used as Basis Spectra for the CLS Model (CHT, Chymotrypsin; HAS, Human Serum Albumin; PHC, Phosphatidyl Choline; CHO, Cholesterol)

	DNA	RNA	ACT	HSA	CHY	COL	GLY	PC	CHO	Protein
DNA	1	0.4060	0.0780	0.0373	0.0271	0.0382	0.0409	0.0060	0.0450	0.0492
RNA		1	0.0232	0.0145	0.0201	0.0690	0.0038	0.0415	0.0220	0.0225
ACT			1	0.8046	0.5251	0.4746	0.1338	0.0972	0.0255	n/a
HSA				1	0.5578	0.5080	0.1542	0.1001	0.0254	n/a
CHY					1	0.2707	0.0661	0.0301	0.0682	n/a
COL						1	0.0908	0.2478	0.0261	n/a
GLY							1	0.0249	0.1373	0.1731
PC								1	0.0191	0.1614
CHO									1	0.0367
Protein										1

Protein = mean protein spectrum based on the 4 proteins: Actin, human serum albumin, chymotrypsin and collagen. |k| is the scalar (dot) product between spectra indicated in the table, where a vector was assigned to each spectrum. |k| values close to 1 indicate the spectra are very similar (therefore hindering accurate CLS analysis) and |k| values <0.1 indicate a high degree of orthogonality (i.e., suitably different).

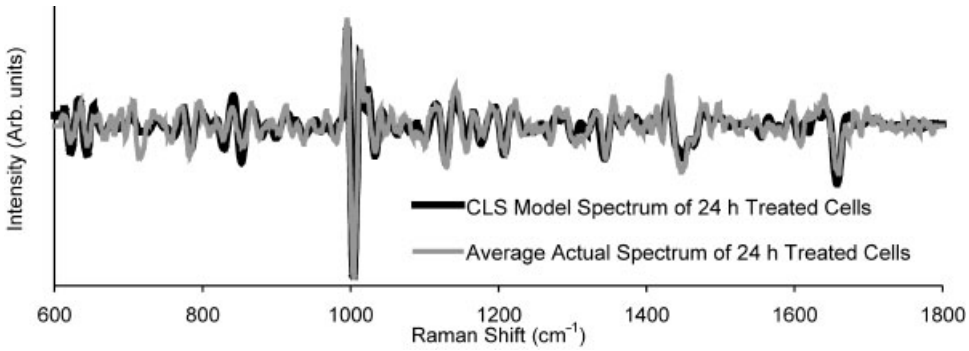

Fig. 3. The CLS predicted model spectrum of 24 h treated cells and average measured 2nd derivative spectrum of all 24 h treated cells.

cells than for treated cells (Fig. 5B). The main variance associated with PC2 is in two regions, namely a large peak at 788/cm (primarily the DNA phosphodiester bond) and a large trough at 1,158/cm (CC stretching in lipids, CN stretching in protein) (Fig. 5A). This confirms that PCA enabled clustering due to DNA degradation and lipid formation as suggested by the CLS analysis.

The MTT assay showed a significant reduction in respiratory activity of the cells over time following exposure to etoposide; namely a reduction of 29.4 and 61.2% after 24 and 48 h respectively (Fig. 6). Western blot analysis determined an increase in p53 in etoposide treated cells, with noticeable differences occurring within 2 h (data not shown).

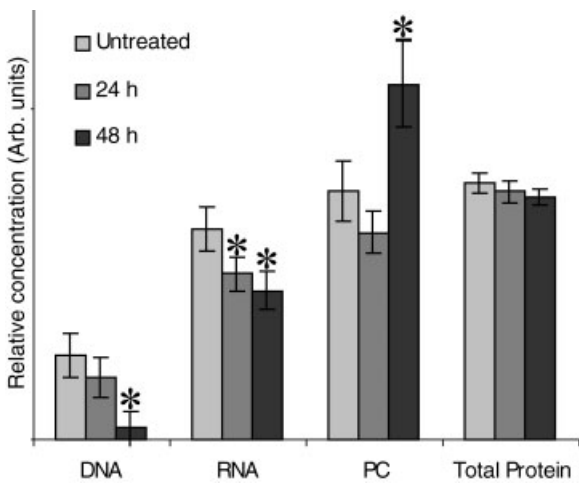

Fig. 4. DNA, RNA, phosphatidyl choline and total protein levels determined with the CLS model with ±1 standard deviation non-biased error bars in A459 cells prior to and following exposure to 100 μM etoposide. Total protein levels have been scaled down by a factor of four for clarity. *Significance is shown relative to untreated controls ($P < 0.05$).

DISCUSSION

This study investigated whether Raman micro-spectroscopy can be used as an effective, label-free, non-invasive method for toxicological testing of living human cells in vitro. Etoposide was selected as a model drug known to inhibit topoisomerase II activity within cells. Etoposide causes the topoisomerase II enzymes to become covalently bound to the DNA causing a blockage to the mitotic enzymatic machinery that attempts to move along the DNA [Hande, 1998]. Hence, etoposide causes DNA fragmentation in specific mitotic phases of the cell cycle where topoisomerase II is expressed. This causes a reduction in phosphodiester bonding.

Etoposide is known to induce apoptosis in cells including A549 [Huang et al., 1997]. Previous biochemical studies of A549 cells performed in our group have shown that etoposide can inhibit the expression of the EGF-R (epidermal growth factor receptor) and cause cytoplasmic retraction and rounding, typical of apoptotic cells, after 4–6 h of etoposide treatment (unpublished data). EGF-R is a receptor tyrosine kinase that is the principal survival factor for lung epithelium, regulating the expression of surfactant protein C and fundamental for differentiation of type II pneumocytes, lung morphogenesis and lung epithelial function.

Changes in cell morphology following exposure to etoposide were consistent with an apoptotic response. The 788/cm peak of DNA, mainly attributed to the OPO backbone of DNA is the clearest observable DNA peak in the raw spectra. This peak decreases between 0 and 24 h and also between 24 and 48 h (Fig. 1A, spectrum b). A decrease is observed between the 24 h

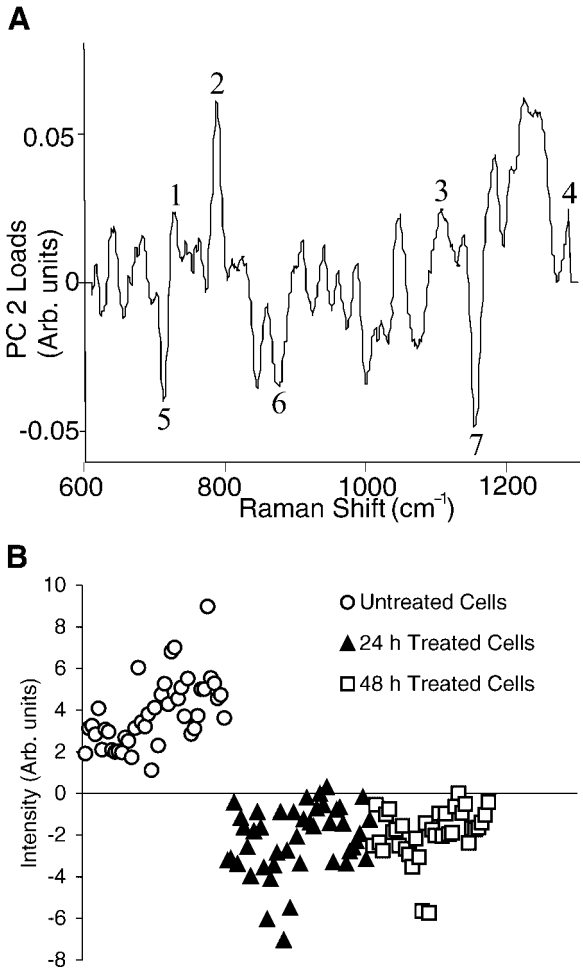

Fig. 5. **A**: Principal component 2 loading. Peaks corresponding to DNA and lipids are indicated. Peaks 1, 2, 3 and 4 relate to peaks that correspond to DNA: 1 = 729/cm (adenine), 2 = 788/cm (OPO stretch of DNA), 3 = 1,094/cm (OPO stretch of DNA) and 4 = 1,283/cm (Thymine and Adenine). Peaks 5, 6 and 7 relate to peaks that correspond to lipids: 5 = 717/cm ($CN^+(CH_3)_3$ stretch), 6 = 877/cm (CCN^+ symmetrical stretch) and 7 = 1,158/cm (CC stretch). **B**: A plot of the principal component 2 scores for the individual cells in the study. The scores for the untreated cells are significantly higher than the treated cells.

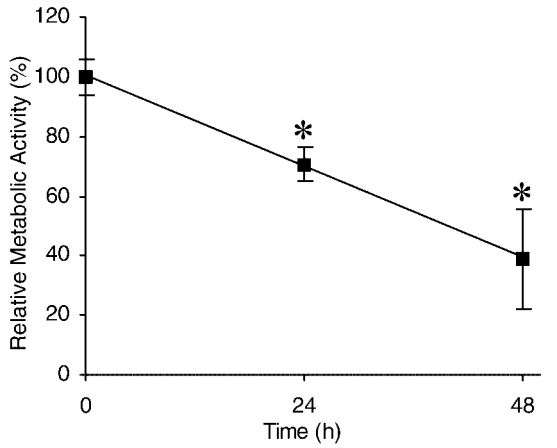

Fig. 6. MTT assay of respiratory activity of A549 cells prior to and following exposure to 100 μM etoposide. *Significance is relative to untreated control ($P < 0.05$). Decrease after 48 h is also significant relative to 24 h metabolic activity.

treated and the untreated spectra in the 788/cm DNA peak region, (Fig. 1B, spectrum b) and an even larger decrease is observed between the 48 h and the untreated spectra (Fig. 1B, spectrum a). This implies that there is continued degradation of DNA after 24 h. This peak is just one of the many biochemical peaks in DNA. With multivariate analysis, the decrease in DNA levels are more accurately evaluated.

CLS analysis of Raman spectra of A549 cells also showed significant decreases in DNA and RNA after 24 and 48 h and increases in lipids after 48 h, consistent with an apoptotic process (Fig. 4) [Notingher et al., 2004b]. PCA was also able to discriminate between treated and untreated cell populations according to variance in DNA degradation and lipid formation (Fig. 5A,B). Cells with advanced apoptosis exhibit significant decreases in RNA after 24 and 48 h as the production of RNA is decreased when DNA becomes fragmented (Fig. 4). In contrast, exposure of cells to a higher dosage of etoposide (250 μM) for 3 or 6 h resulted in only insignificant reductions in DNA or RNA concentration as determined with the CLS model (Fig. S-1). This observation is not surprising in light of the fact that the doubling time of A549 cells has been determined through experience to be approximately 32 h and etoposide will only cause DNA fragmentation during mitosis. This implies that the cell: drug interaction time is a more critical factor than drug strength. Raman spectroscopy could easily be used in this way to evaluate the concentration of drug required to take effect at the cellular level.

DNA repair mechanisms may also be working to revert the damage at this stage and an increase in the activity of transmembrane pumps to remove the drug from the cell may impart a degree of drug resistance at these earlier time points [McKeegan et al., 2003]. MTT assay, in contrast, revealed a significant decrease in respiratory activity after 2 h of etoposide treatment (Fig. S-2). This difference may be because the MTT assay is a measure of mitochondrial activity within the cell as

opposed to nuclear activity. Since mitochondria exist within the cell at various stages of their replication cycle, independently of the cell cycle, their replicating DNA (which accounts for less than 1% of the total cellular DNA) can be immediately targeted by etoposide [Alberts et al., 2002].

Phospholipid and cholesterol levels are generally thought to remain constant in etoposide treated cells [Horiuchi et al., 2002]. The CLS spectral analysis, however, revealed a significant increase in the amount of phosphatidyl choline (our model lipid) at the 48 h time point. This is evident by the increase in the 1,158 and 720/cm peaks, relating to CC stretching in lipids and the symmetric stretching of the choline group $CN^{+}(CH_3)_3$ in phosphatidyl choline (Fig. 1A). Increased phosphatidyl choline may relate to an increase in vesicle production. Animal cells produce small single-membrane bound vesicles for the purpose of removing cellular waste and toxins by exocytosis [Alberts et al., 2002]. Following 48 h exposure to etoposide, the concentration of phosphatidyl choline increased significantly (by 43.0%), suggesting the production of many such intracellular vesicles (confirmed by optical microscopy).

Damage to DNA was confirmed by monitoring p53 levels using Western blotting. p53 is a tumour-suppressor that works by binding to DNA and stimulating the production of p21, which in turn interacts with a cell division-stimulating protein (cdk2) to prevent the cell becoming mitotic. Levels of p53 increase, as observed here, in response to DNA fragmentation and cellular distress signals in order to prevent abnormal cell proliferation [O'Reilly et al., 2001; N.C.B.I., 2003]. Apoptosis of the cells following DNA fragmentation was also associated with a lower respiratory activity for the cells as monitored by MTT assay, with decreases of 29.4 and 61.2% observed after 24 and 48 h exposure to etoposide (Fig. 6).

Raman spectroscopy, when combined with the analytical methods presented, is a powerful tool for cellular analysis and in vitro toxicological testing on human cells. It offers the opportunity to enhance the understanding of how chemicals react with human cells in real time and may find applications in the toxicology screening of other drugs, chemicals and new biomaterials, with a range of cell types. This research also supports the goal of an alternative testing system that reduces economic cost and increases throughput without animal testing, as stipulated by the EU [(E.C.), 2001].

REFERENCES

Alberts B, Johnson A, Lewis J, Raff M, Roberts K, Walter P. 2002. Molecular biology of the cell. Garland Sci 4th Ed. pp 757–765.

Barnes RJ, Dhanoa MS, Lister SJ. 1989. Standard normal variate transformation and de-trending of near-infrared diffuse reflectance spectra. Appl Spectrosc 43: 772–777.

Caspers PJ, Lucassen GW, Carter EA, Bruining HA, Puppels GJ. 2001. In vivo confocal Raman microspectroscopy of the skin: Noninvasive determination of molecular concentration profiles. J Invest Dermatol 116:434–442.

(E.C.). 2001. WHITE PAPER: Strategy for a Future Chemicals Policy Brussels: Commission of the European Communities, pp 4–32.

Hande KR. 1998. Etoposide: Four decades of development of a topoisomerase II inhibitor. Eur J Cancer 34:1514–1521.

Hawi SR, Nithipatikom K, Wohlfeil ER, Adar F, Campbell WB. 1997. Raman microspectroscopy of intracellular cholesterol crystals in cultured bovine coronary artery endothelial cells. J Lipid Res 38:1591–1597.

Horiuchi A, Yasugi E, Iwasaki C, Fujimoto K, Oshima M. 2002. Changes in cell membrane and cellular lipids in apoptotic cells induced by dolichyl phosphate differ from findings in cells induced by etoposide. J Oleo Sci 51: 35–42.

Huang Y, Chan AML, Liu Y, Wang X, Holbrook NJ. 1997. Serum withdrawal and etoposide induce apoptosis in human lung carcinoma cell line A549 via distinct pathways. Apoptosis 2:199–206.

Jell G, Notingher PL, Notingher I, Tsigkou O, Polak JM, Hench L, Stevens MM. In situ spectral monitoring of foetal bone cell differentiation upon exposure to Bioglass dissolution ions. (2006, under review).

Krafft C. 2004. Bioanalytical applications of Raman spectroscopy. Anal Bioanalytical Chem 378:60–62.

Krafft C, Knetschke T, Funk RHW, Salzer R. 2005. Identification of organelles and vesicles in single cells by Raman microspectroscopic mapping. Vib Spectrosc 38:85–93.

Laemmli UK. 1970. Cleavage of structural proteins during the assembly of the head of bacteriophage. Nature 227:680–685.

Lazarou J, Pomeranz BH, Corey PN. 1998. Incidence of adverse drug reactions in hospitalized patients—A meta-analysis of prospective studies. JAMA 279:1200–1205.

Luypaert J, Heuerding S, Vander Heyden Y, Massart DL. 2004. The effect of preprocessing methods in reducing interfering variability from near-infrared measurements of creams. J Pharm Biomed Anal 36:495–503.

Maquelin K, Choo-Smith LP, Endtz HP, Bruining HA, Puppels GJ. 2002. Rapid identification of Candida species by confocal Raman micro spectroscopy. J Clin Microbiol 40:594–600.

McKeegan KS, Borges-Walmsley MI, Walmsley AR. 2003. The structure and function of drug pumps: An update. Trends Microbiol 11:21–29.

Moore TJ, Psaty BM, Furberg CD. 1998. Time to act on drug safety. JAMA 279:1571–1573.

N.C.B.I. 2003. Genes and Disease: Cancers: The p53 tumor suppressor protein.

Notingher I, Verrier S, Haque S, Polak JM, Hench LL. 2003. Spectroscopic study of human lung epithelial cells (A549) in culture: Living cells versus dead cells. Biopolymers 72:230–240.

Notingher I, Bisson I, Bishop AE, Randle WL, Polak JMP, Hench LL. 2004a. In situ spectral monitoring of mRNA translation in embryonic stem cells during differentiation in vitro. Anal Chem 76:3185–3193.

Notingher I, Green C, Dyer C, Perkins E, Hopkins N, Lindsay C, Hench LL. 2004b. Discrimination between ricin and sulphur mustard toxicity in vitro using Raman spectroscopy. J R Soc Interface 1:79–90.

Notingher I, Jell G, Lohbauer U, Salih V, Hench L. 2004c. In situ non-invasive spectral discrimination between bone cell phenotypes used in tissue engineering. J Cell Biochem 92:1180–1192.

O'Reilly MA, Staversky RJ, Watkins RH, Reed CK, Jensen KLD, Finkelstein JN, Keng PC. 2001. The cyclin-dependent kinase inhibitor p21 protects the lung from oxidative stress. Am J Respir Cell Mol Biol 24:703–710.

Puppels GJ, Demul FFM, Otto C, Greve J, Robertnicoud M, Arndtjovin DJ, Jovin TM. 1990. Studying single living cells and chromosomes by confocal Raman microspectroscopy. Nature 347:301–303.

Raman CV, Krishnan KS. 1928. A new type of secondary radiation. Nature 121:501–502.

RPSGB. 2002. Martindale—The complete drug reference, 33rd edition. London: Pharmaceutical Press.

Salenius JP, Brennan JF, Miller A, Wang Y, Aretz T, Sacks B, Dasari RR, Feld MS. 1998. Biochemical composition of human peripheral arteries examined with near-infrared Raman spectroscopy. J Vasc Surg 27:710–719.

Shafer-Peltier KE, Haka AS, Fitzmaurice M, Crowe J, Myles J, Dasari RR, Feld MS. 2002. Raman microspectroscopic model of human breast tissue: Implications for breast cancer diagnosis in vivo. J Raman Spectrosc 33: 552–563.

Takai Y, Masuko T, Takeuchi H. 1997. Lipid structure of cytotoxic granules in living human killer T lymphocytes studied by Raman microspectroscopy. Biochim Biophys Acta Gen Subjects 1335:199–208.

Uzunbajakava N, Lenferink A, Kraan Y, Volokhina E, Vrensen G, Greve J, Otto C. 2003a. Nonresonant confocal Raman imaging of DNA and protein distribution in apoptotic cells. Biophys J 84:3968–3981.

Uzunbajakava N, Lenferink A, Kraan Y, Willekens B, Vrensen G, Greve J, Otto C. 2003b. Nonresonant Raman imaging of protein distribution in single human cells. Biopolymers 72:1–9.

Verrier S, Notingher I, Polak JM, Hench LL. 2004. In situ monitoring of cell death using Raman microspectroscopy. Biopolymers 74:157–162.